galaxies

MDPI

Article

Knots in Relativistic Transverse Stratified Jets

Zakaria Meliani [1,*,†] and Olivier Hervet [2,†]

[1] LUTH, Observatoire de Paris, PSL Research University, CNRS, Université Paris Diderot, Sorbonne Paris Cité, 5 place Jules Janssen, 92195 Meudon, France

[2] Santa Cruz Institute for Particle Physics and Department of Physics, University of California at Santa Cruz, Santa Cruz, CA 95064, USA; ohervet@ucsc.edu

* Correspondence: zakaria.meliani@obspm.fr; Tel.: +33-14507-7425

† These authors contributed equally to this work.

Academic Editors: Markus Boettcher; Emmanouil Angelakis and Jose L. Gómez

Received: 16 July 2017; Accepted: 21 August 2017; Published: 5 September 2017

Abstract: We investigate the plasmoid knot formation in stratified relativistic jet by means of relativistic magneto-hydrodynamics simulations. Indeed, astrophysical jets in active galactic nuclei (AGN) seem to be transversely stratified, with a fast inner jet and a slower outer jet. It is likely that the launching mechanism for each component is different. On the other hand, the steady and moving knots' properties are observed along these jets. With the proposed model, we were able to link the different types of observed knot in various radio loud AGN with specific stratified jet characteristics. We showed that the increase energy flux at the outer edge of the jet induces a steady knot near the core and a moving knot at a greater distance.

Keywords: AGN; relativistic jet; magnetohydrodynamics simulation.

1. Introduction

There is growing evidence of transverse stratification of relativistic astrophysical jets with clear indication of a fast inner jet (spine) embedded in a slower outer flow (layer). In many active galactic nuclei (AGN), a limb-brightened jet morphology is observed on pc scales [1], which is interpreted as an outcome of the differential Doppler boosting between the jet spine and layer [2]. This scenario is supported by multiple radio-load AGN observations, such as the well-known radio galaxy M87, which presents hints of a two-component jet from its polarized emission [3].

Numerous standing and moving radio knots in AGN jets have been observed over the last decades in very long baseline interferometry (VLBI) thanks to dedicated long-term monitoring programs such as MOJAVE (http://www.physics.purdue.edu/MOJAVE/) or TANAMI (http://pulsar.sternwarte.uni-erlangen.de/tanami/). From these observations, stationary knots are often interpreted as re-collimation shocks resulting from the propagation of overpressured super-Alfvenic jets through the external medium. This pressure difference between the jet and the external medium is caused by the large distances covered by relativistic AGN jets in the galactic medium. Indeed, with distance, the external medium pressure decreases faster than the jet pressure, which gives rise to rarefaction waves and shock waves within the jet. This phenomena was studied using the characteristic methods [4].

In order to study the effects of the jet transverse stratification, we elaborate a two-component jet model according to the jet formation scenarios [5–7] and numerical simulation [8]. We adopt a two-component jet model with various kinetic energy flux distributions between the inner–outer jets [9]. We aim to investigate how this energy distribution influences the overall jet stability, the re-collimation shock development, and the local jet acceleration. Additionally, we assume various configurations. The first case is an overpressured uniform jet propagating in the external medium. In all the other investigated cases, we set a transverse structured jet with an overpressured inner jet. This assumption results from the intrinsic properties of the launching region, as described above.

2. Model

To study re-collimation shocks in transverse stratified jets, we adopt a two-component jet model with two uniform components. The model uses the basic characteristics of relativistic AGN jets, such as the total kinetic luminosity flux within an interval $L_{\rm k} = \left[10^{43}, 10^{46}\right]$ ergs/s [10], and the outer radius of the two-component jet $R_{\rm out} = R_{\rm jet} \sim 0.1$ pc at a parsec scale distance from the black hole. For the less-constrained inner jet radius, we adopt the initial value $R_{\rm in} = R_{\rm jet}/3$. As initial condition for simulations, we establish a cylindrical flow column along the jet axis with a radius $R_{\rm jet}$. Two types of jets are investigated in this paper: uniform jets (the reference case) and two-component jets. For structured jets, we have a discontinuity in the density, pressure, and velocity at the interface of the two components $R_{\rm in}$. The jet properties are related to the external medium density and pressure by

$$\rho = \begin{cases} \rho_0 \ \eta_{\rho,\rm in} & R \leq R_{\rm in}\,, \\ \rho_0 \ \eta_{\rho,\rm out} & R_{\rm in} < R < R_{\rm jet}\,, \end{cases} \quad \text{and} \quad p = \begin{cases} p_0 \ \eta_{p,\rm in} & R \leq R_{\rm in}\,, \\ p_0 \ \eta_{p,\rm out} & R_{\rm in} < R < R_{\rm jet}\,. \end{cases} \tag{1}$$

where ρ_0 and p_0 are, respectively, the density and the pressure of the external medium, $\eta_{\rho,\rm in}$ and $\eta_{\rho,\rm out}$ are the inner and outer jet density ratio relative to the external medium density, and $\eta_{p,\rm in}$ and $\eta_{p,\rm out}$ are the inner and outer jet pressure ratio relative to the external medium pressure.

Six cases (A, B, C, D, E, and F) were investigated. The first case (A) presents a uniform jet with a Lorentz factor $\gamma = 10$. All the other cases are two-component jet simulations; their order follows an increasing ratio of the outer/inner jets component kinetic powers. Hence, case (B) has the most powerful inner jet, carrying 95% of the total kinetic power. Cases (C) and (D) are set with inner and outer jets carrying relatively the same order of kinetic power. In case (E), the jet is set with very powerful outer jet carrying 99.93% of the total kinetic power; this is also the only case where the outer jet is denser than the external medium. In the last case (F), the inner jet is empty and all energy is carried by the outer jet. All these cases are listed in Table 1. We should notice that the increase in the outer jet component's kinetic energy flux induces an increase of its density and thus a decrease in the sound speed; as a result, the Mach number of the outer jet component in cases C, D, E increases.

Table 1. Most relevant parameters for the two models investigated, the density ratio η_ρ, the Mach number $\mathcal{M}_{\rm c}$, the contribution of each jet components to the total kinetic energy flux of the jet $L_{\rm k,\,in}/L_{\rm k,\,total}$, $L_{\rm k,\,out}/L_{\rm k,\,total}$. In addition to these values, the external medium has a normalized number density $\rho_0 = 1$ and a normalized pressure $p_0 \simeq 5 \times 10^{-2}$ or $p_0 \simeq 1 \times 10^{-3}$ (these two types of pressure are chosen according to the energy ratio between inner and outer jet components). The inner jet always presents an initial Lorentz factor of $\gamma = 10$—higher than that of the outer jet initialized at $\gamma = 3$. The outer jet is assumed to be in pressure equilibrium with the external medium $\eta_{p,\,\rm out} = 1$, contrary to the inner jet which presents a larger pressure $\eta_{p,\,\rm in} = 1.5$.

	Inner Jet		**Outer Jet**		**Structured Jet**		
Case	$\eta_{\rho\,,\rm in}$	$\mathcal{M}_{\rm c,in}$	$\eta_{\rho\,,\rm out}$	$\mathcal{M}_{\rm c,out}$	$L_{\rm k,\,in}/L_{\rm k,\,total}$	$L_{\rm k,\,out}/L_{\rm k,\,total}$	**Two-Component Jet**
A	4.5×10^{-4}	1.22			1	0.0	No
B	5×10^{-1}	4.34	5×10^{-6}	1.16	0.95	0.05	Yes
C	5×10^{-3}	1.22	5×10^{-1}	16.34	0.70	0.30	Yes
D	5×10^{-6}	1.22	1×10^{-1}	6	0.25	0.75	Yes
E	5×10^{-3}	1.22	5×10	19.0	5×10^{-3}	0.995	Yes
F	1×10^{-3}	0	5×10^{-2}	6.0	0	1	Yes

3. Results and Discussion

Our transverse structured jet model shows that energy distribution between the inner and the outer jet could be the key to jet classification (Figure 1). Indeed, the energy distribution has a significant influence on the formation, the state of internal shocks, and on the local jet acceleration. The model

we propose here shows how the jet structure affects the development of the stationary and the non-stationary shocks observed in AGN jets. The jet structures modify the configuration of the internal shocks and the accelerations in the rarefaction regions. This structure can result from the jet launching mechanism.

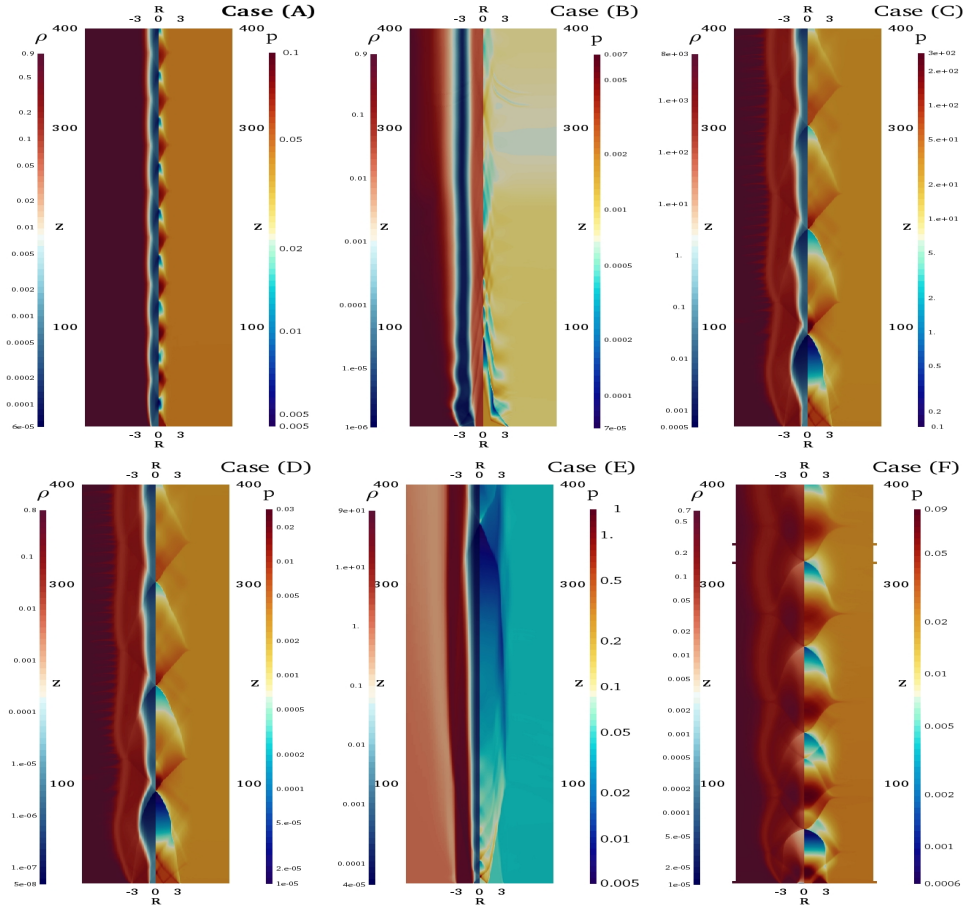

Figure 1. Two-dimensional view of all the simulated cases of the jets along the poloidal direction. In each figure, the density color bar is drawn on the left side and the pressure color bar on the right side. The jet figures are stretched in the radial direction and squeezed in the longitudinal direction.The distance R and Z and in unit of the inner jet radius.

We can classify the relativistic structured jets according to the transverse energy distribution between the two components as follows. This distribution affects the transverse variation Mach number, since the density between the two components is related to the energy flux within each component.

The jets with low-energy outer jet (case B) show weak shocks. Moreover, the rarefaction waves are inefficient at accelerating the jet. The outer jet plays the role of a shear layer isolating the inner jet from the external medium. Moreover, the low inertia of the outer component allows it to absorb waves. This makes a more efficient energy transfer from the inner to the outer jet. The Lorentz factor of the outer component increases with distance. Overall, the inner jet's Lorentz factor remains near the initial values.

The jets with near-equal energy distribution between the two components (cases C and D) show two shock wave structures with different wavelengths.

In case (D), the Lorentz factor reaches locally $\gamma \sim 30$ and even $\gamma \sim 50$. This acceleration is the result of the energy transfer from the outer to the inner jet by the inward propagating rarefaction

waves that rise at the edge of the outer jet. The large difference in the Mach number between the hot inner jet and cold outer jet increases the efficiency of the energy transfer from outer to inner jet.

The jet with large energy carried by the outer jet (such as in case (E); Figure 1) could be representative of a jet with steady knots near the core and moving features at large distances like those observed in some sources. In the region with the steady shocks, the jet radius remains relatively constant, but downstream this radius increases with distance. The jet expansion at large distance is the result of the large inertia of the outer jet that propagates in a rarefied external medium.

The last case (F) shows that jets with empty spines could evolve to conical shapes under the influence of the internal shocks.

These simulations show that the transverse structure in relativistic jets could be responsible for the diversity in knots observed in radio sources.

Acknowledgments: Part of this work was supported by the PNHE and Observatoire de Paris. This work acknowledges financial support from the UnivEarthS Labex program at Sorbonne Paris Cité (ANR-10-LABX-0023 and ANR-11-IDEX-0005-02). O.H. thanks the U.S. National Science Foundation for support under grant PHY-1307311 and the Observatoire de Paris for financial support with ATER position. All the computations made use of the High Performance Computing OCCIGEN and JADE at CINES within the DARI project c2015046842. This research has made use of data from the MOJAVE database that is maintained by the MOJAVE team [11].

Author Contributions: Z.M. contributed to the development of the two-component model and numerical simulation with AMRVAC code. O.H. contributed to the development of the two-component model and link with observations.

Conflicts of Interest: The authors declare no conflict of interest.

References

1. Giroletti, M.; Giovannini, G.; Feretti, L.; Cotton, W.D.; Edwards, P.G.; Lara, L.; Marscher, A.P.; Mattox J.R.; Piner, B.G.; Venturi, T. Parsec Scale Properties of Markarian 501. *Astrophys. J.* **2004**, *600*, 127–140.
2. Giovannini, G. The radio jet velocities at high resolution. *New Astron. Rev.* **2003**, *47*, 551–555.
3. Attridge, J.M.; Roberts, D.H.; Wardle, J.F.C. Radio Jet-Ambient Medium Interactions on Parsec Scales in the Blazar 1055+018*. *Astrophys. J.* **1999**, *518*, 87.
4. Daly, R.A.; Marscher, A.P. The gasdynamics of compact relativistic jets. *Astrophys. J.* **1988**, *334*, 539–551.
5. Blandford, R.D.; Payne, D.G. Hydromagnetic flows from accretion discs and the production of radio jets. *Mon. Not. R. Astron. Soc.* **1982**, *199*, 883–903.
6. Blandford, R.D.; Znajek, R.L. Electromagnetic extraction of energy from Kerr black holes. *Mon. Not. R. Astron. Soc.* **1977**, *179*, 433–456.
7. Meliani, Z.; Sauty, C.; Vlahakis, N.; Tsinganos, K.; Trussoni, E. Nonradial and nonpolytropic astrophysical outflows VIII. A GRMHD generalization for relativistic jets. *Astron. Astrophys.* **2006**, *447*, 797–812.
8. McKinney, J.C.; Blandford, R.D. Stability of relativistic jets from rotating, accreting black holes via fully three-dimensional magnetohydrodynamic simulations. *Mon. Not. R. Astron. Soc.* **2009**, *394*, L126–L130.
9. Hervet, O.; Meliani, Z.; Zech, A.; Boisson, C.; Cayatte, V.; Sauty, C.; Sol, H. Shocks in relativistic transverse stratified jets, a new paradigm for radio-loud AGN. *arXiv* **2017**, arXiv:astro-ph/1705.10556.
10. Rawlings, S.; Saunders, R. Evidence for a common central-engine mechanism in all extragalactic radio sources. *Nature* **1991**, *349*, 138–140.
11. Lister, M.L.; Cohen, M.H.; Homan, D.C.; Kadler, M.; Kellermann, K.I.; Kovalev, Y.Y.; Ros, E.; Savolainen, T.; Zensus, J.A. MOJAVE: Monitoring of Jets in Active Galactic Nuclei with VLBA Experiments. VI. Kinematics Analysis of a Complete Sample of Blazar Jets. *Astron. J.* **2009**, *138*, 1874–1892.